

## Specific Aims

The development and proliferation of quantitative image analysis methods have accelerated research efforts and are having an increasingly significant impact in modern clinical practice. Although the research utility of these techniques has been amply demonstrated in determining longitudinal and groupwise trends, they are also becoming increasingly relevant in the clinical setting in providing biomarkers for aiding patient diagnoses, monitoring disease progression, and determining treatment outcomes. Increases in the capabilities and accessibility of computational facilities and a corresponding sophistication in computational algorithms have only made such practices more commonplace.

One of the most significant hurdles in adopting more quantitative clinical practices and exploring additional novel research pathways is the availability of accurate, robust, and easy-to-use image analysis tools. Historically, the research and clinical communities (and their overlap) have significantly benefited from the development and proliferation of imaging-related analysis packages, particularly those softwares which have been tailored for specific application domains. Although several such established packages exist for neuroimaging research (e.g., FSL, FreeSurfer, AFNI, SPM), no such package exists for pulmonary imaging analysis. The primary goal of this proposal is to develop a robust, open-source image analysis toolkit and dissemination platform specifically targeted at the pulmonary research community.

Although methodological research is continually being presented at conferences and published in various venues, the unfortunate reality is that much of this work exists strictly in “advertisement” form. Oftentimes the underlying code is unavailable to other researchers or is implemented in a limited manner (i.e., strictly as proof-of-concept software). Frequently, crucial parameter choices are omitted in the corresponding publication(s) which makes external implementations difficult. In addition, the data used to showcase the proposed methodologies are often private and actual data visualization is limited to carefully selected snapshots for publication (i.e., advertisement) purposes which might not be representative of algorithmic performance. Finally, many of these analysis methods are patented and/or integrated into proprietary commercial software packages which severely limits accessibility to researchers.

As a corrective alternative, this proposal will provide an open-source software toolkit targeted for pulmonary research. As principal developers of the popular, open-source ANTs (Advanced Normalization Tools) package, we have extensive experience in the development of well-written software that has gained much traction in the neuroscience community and propose to make a similar impact in the pulmonary community with this proposal. Specifically, we plan to provide methods for core pulmonary image analysis tasks across multiple modalities, many of which we have proposed previously in past publications. These basic tasks include pulmonary image registration, template building for cross-sectional and longitudinal (i.e., respiratory cycle) analyses, functional and structural lung image segmentation, and computation of quantitative image indices as potential imaging biomarkers. In addition to the software, we will provide additional data, documentation, and tutorial materials consistent with open-science principles. Formally, this proposal is defined by the following specific aims:

- **Specific Aim 1: Develop a set of open-source software tools for CT, proton, and He-3 pulmonary computational analysis.** These open-source software tools will specifically target pulmonary image analysis and comprise core application functions such as inspiratory/expiratory registration for inferring pulmonary kinematics, ventilation-based segmentation, lung and lobe estimation, airway segmentation, and calculation of clinical indices for characterization of lung development and pathology. To maximize usability, much (if not all) of the actual code will be developed and distributed within the Insight Toolkit of the National Library of Medicine.
- **Specific Aim 2: Provide multiple sets of multi-modal annotated lung data (CT, proton, and He3) for unrestricted public use.** In addition to the public unavailability of the algorithms used to produce the results discussed in certain publications, the input and output data is also typically not available. Such availability would be invaluable to other researchers in the community for appropriation for their own purposes including algorithmic performance assessment and running the proposed prior-based methods requiring annotated input data.
- **Specific Aim 3: Evaluate and disseminate the developed resources by leveraging input data from multiple partner investigators.** This aim will evaluate and refine the developed methodology within the real-world context of pulmonary research being carried out at various partner sites (e.g., University of Virginia, University of Pennsylvania, ..., need to add others). We will disseminate the results of the project through open-source distribution of the software, data and write-ups, online user support, and conduct of hands-on training workshops.

# ITK-Lung: A Software Framework for Lung Image Processing and Analysis

## Research Strategy

### 3(a) Significance

The increased utilization of imaging for both research and clinical purposes has furthered the demand for quantitative image analysis techniques. The use of these computational techniques are motivated by the need for less subjectivity and more standardization in medical image interpretation, increased speed and automation in diagnosis, and greater robustness and accuracy for determining biological correlates with imaging findings. For example, in the area of pharmaceutical development and testing, imaging biomarkers are crucial. In order to determine fundamental study parameters such as drug safety and effectiveness, quantitative assessments derived from imaging measures must be objective and reproducible [1] which is often difficult without computational aid given the intra- and inter-reader variability in radiological practice [2, 3]. Additionally, the exciting possibilities associated with “big data” and the potential for improvement in individualized, evidence-based medicine has also increased the need for sophisticated data transformation and machine learning techniques.

Well-vetted and publicly available software is a significant benefit to targeted research communities. For example, the neuroscience community has greatly benefited from highly evolved software packages such as FreeSurfer [4], the FMRIB Software Library (FSL) [5], the Analysis of Functional NeuroImages (AFNI) package [6], and the Statistical Parametric Mapping (SPM) package [7]. Performing a pubmed query for any one of these softwares every year for the past decade (cf Figure 1) illustrates the growing use of such packages and the research studies that are produced as a result. However, despite the absolute number of articles produced using such software and the year-by-year usage increase, no such analogous set of tools exist for pulmonary-specific research. In fact, in a recent review of CT- and MRI-derived biomarkers for pulmonary clinical investigation, the authorial consensus is that “universally available image analysis software” is a major hinderance to more widespread usage of such imaging biomarkers [8].

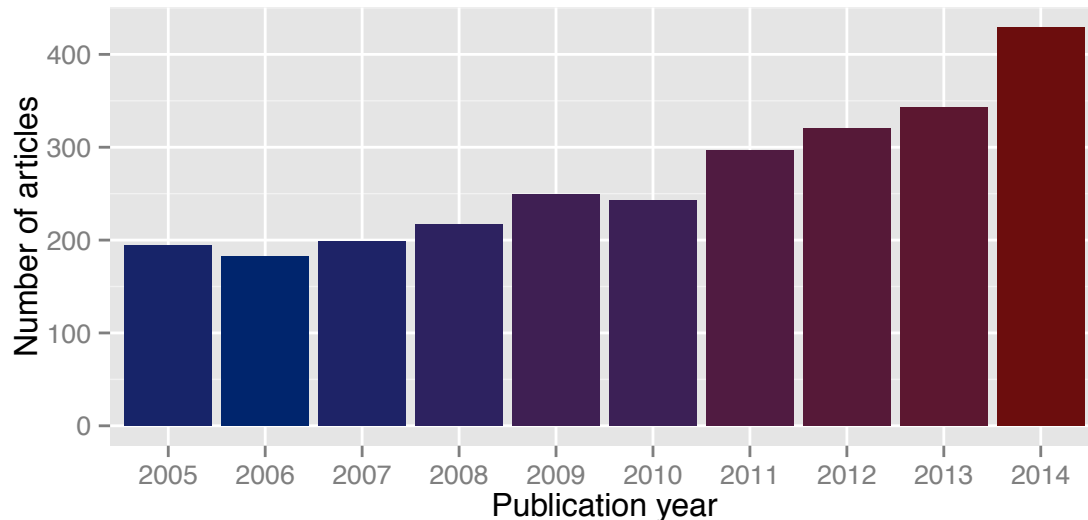


**Figure 1:** Number of articles per year which cite publicly available neuroimaging analysis packages (specifically, FreeSurfer, AFNI, FSL, and SPM). Although the benefits seem clear for the neuroscience community, analogous efforts within the pulmonary community have yet to be undertaken despite consensus amongst researchers and clinicians regarding the utility of such offerings.

Medical image analysis libraries (e.g., the NIH-sponsored Insight ToolKit) provide extensive algorithmic capabilities for a range of generic image processing tasks. However, tailored software packages for certain application domains (e.g., lung image analysis) are not available despite the vast number of algorithms that have been proposed in the literature. Note that the goals of this proposal would significantly support the National Library of Medicine’s own open-source directives in that all software would be developed using the established Insight ToolKit’s coding and testing standards with the eventual idea that much (if not all)

of the actual code would be contributed for inclusion in future versions of the Insight ToolKit as we have done in the past. It should also be noted that open-source software, in general, has documented benefits within the targeted communities for which it is developed and supported. In addition to the increase in research output illustrated earlier, open-source permits students and researchers to learn specific computational techniques in a social environment [9]. This, in turn, provides motivation for user-based support including potential contributions such as bug fixes and feature additions. Additional analyses have shown the tremendous cost savings that open-source software yields [10]. Furthermore, it should be highlighted that open-source development and distribution within a large, and well-invested community (such as ITK) takes advantage of Linus's law, i.e., "given enough eyeballs, all bugs are shallow," for producing robust software.

### **3(b) Innovation**

#### **3(b.1) Open source pulmonary algorithmic innovation**

Given the lack of open-source solutions for pulmonary image analysis, the proposal goals would produce an innovative platform for performing such research. Similar to the brain-specific algorithms provided in our ANTs toolkit, our novel and useful proposal would include the most essential algorithms for analyzing lung images from different modalities including CT, <sup>3</sup>He, and proton MRI. Many algorithms have been proposed in various technical venues but that which we propose would provide well-vetted and easy-to-use implementations of specific robust methodologies for pulmonary medical image analysis, many of which have been developed by our group. To facilitate the usage of these algorithms, we will provide several self-contained online examples (complete with data).

#### **3(b.2) Publicly available multi-site data as a reproducible and didactic component**

An additional innovative component we are proposing is the inclusion of complete study data and detailed instructions for generating reproducible, multimodality pulmonary studies using the proposed package with input data from several of our external collaborators and colleagues. Specifically, we have asked several scientists and researchers who are familiar with our work to provide imaging data of various modalities which we will then process using the proposed toolkit. These processed data will then not only be returned to the corresponding providers with detailed instructions on reproducing these results in their own labs but will also be provided to the public for any interested researcher to reproduce the results. Given the different image acquisition sources, this strategy should also demonstrate the robustness of our tools.

Included in these analyses will be analyses of our own data. Any clinical findings of interest will be published in traditional venues (e.g., Chest). In addition, we will provide all image data and the quantitative analysis scripts as a companion release to accompany the paper (e.g., see previous similar offerings from our group [11, 12]). Such a comprehensive clinical investigation using these tools will not only provide insight into the specifics of certain pulmonary pathologies but will also provide a reproducible mechanism for using the tools created with this proposal.

### **3(c) Research design**

#### **3(c.1) Preliminary data**

##### **3(c.1.1) Generic ANTs core tools for image analysis and processing**

Many of the core programs comprising portions of the proposed pulmonary software framework have been created and made available within ANTs (and either simultaneously or subsequently made available in ITK). However, as mentioned earlier, these programs have more general application and require pulmonary-specific tuning for the tasks targeted by this proposal. The following list comprises these core software tools for tuning, subsequent extensions, documentation, tutorial generation, and the creation of easy-to-use bash scripts for large-scale processing of pulmonary imaging data:

**ANTs image registration.** One of the most important methodological developments in medical image analysis is the advent of image registration techniques capable of accommodating the highly complex inter-individual variations seen in human neuroanatomy. Our team is well-recognized for seminal contributions to the field that date back to the original elastic matching method of Bajcsy and co-investigators [13–15]. Our most recent work, embodied in the ANTs open-source, cross-platform

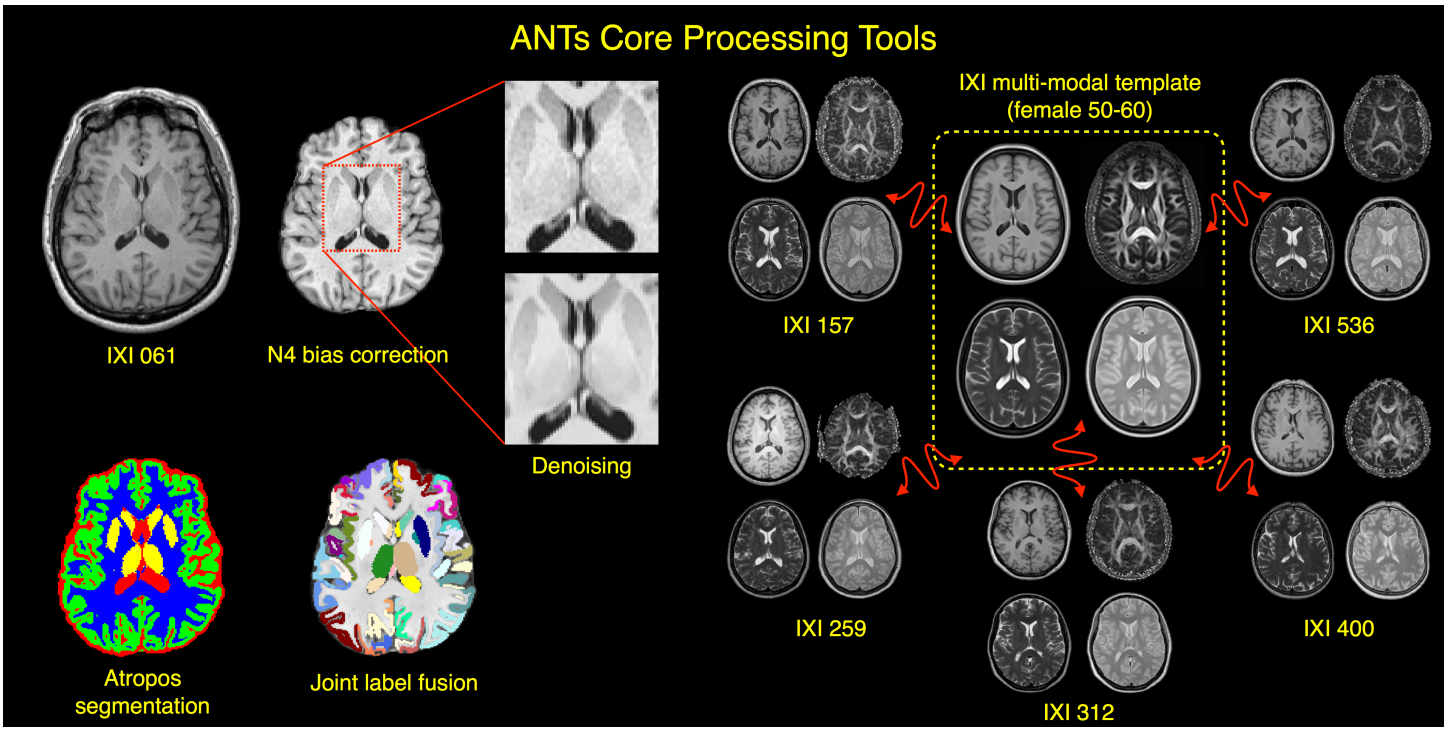


Figure 2: Core processing tools that have made the ANTs package one of the most popular neuroimaging toolkits. Fundamental processing tasks such as image registration, template generation, bias correction, denoising, intensity-based segmentation, and joint label fusion are extremely well-performing software components which have been utilized for neuroimaging tasks such as brain extraction and cortical thickness estimation.

toolkit for multiple modality image processing, continues to set the standard in the field. ANTs not only encodes the most advanced results in registration research, notably the Symmetric Normalization (SyN) algorithm for diffeomorphisms [16], but also packages these within a full featured platform that includes an extensive library of similarity measures, transformation types, and regularizers. Recently, a thorough comparison with the original SyN algorithm was performed using a B-spline variant [11]. This evaluation utilized multiple publicly available, annotated brain data sets and demonstrated statistically significant improvement in label overlap measures. As part of that study, we produced the scripts `antsRegistrationSyN.sh` and `antsRegistrationSyNQuick.sh` which provide a simple interface to our normalization tools for brain-specific normalization.

**Multi-modal template generation.** Given the variability in anatomical shape across populations and the lack of publicly available atlases for specific organs, generating population- or subject-specific optimal shape/intensity templates significantly enhances study potential [17, 18]. First, an average template is estimated via a voxel-wise mean of all the individual subject images. This estimate is iteratively updated by registering each image to the current template, performing a voxelwise average to create a new estimate, and then “reshaping” this template based on the average inverse transformation which “moves” the template estimate closer to the group mean. See Figure 2 for a cohort-specific multi-modal brain template for females in the age range 50–60. This functionality has proven to be a vital component of the ANTs toolkit for performing neuroimaging research (e.g., [???, 12, 19–22]).

**Bayesian-based segmentation with spatial and MRF priors.** Early statistically-based segmentation work appropriated NASA satellite image processing software for classification of head tissues in 2-D MR images [23]. Following this work, many researchers adopted statistical methods for  $n$ -tissue anatomical brain segmentation. The Expectation-Maximization (EM) framework is natural [24] given the “missing data” aspect of this problem. The work described in [25] was one of the first to use EM for finding a locally optimal solution by iterating between bias field estimation and tissue segmentation. Core components of this type of work is the explicit modeling of the tissue intensity values as statistical distributions [26, 27] and the use of MRF modeling [28] for regularizing the classification results [29]. Recently, researchers have begun to rely on spatial prior probability maps of anatomical structures of interest to encode domain knowledge [30, 31] by providing spatial prior probability maps and an initial segmentation. Although this particular segmentation framework has significant application in the neuroimaging domain, it has also applicable to other domains such as breast MRI [32, 33] and functional ventilation of the

lung [34]. However, despite the numerous algorithms and other developments which have been proposed over the years, there are an extremely limited number of software implementations to perform these types of segmentations. This deficit inspired us to create our own Bayesian-based segmentation framework [35] (denoted as Atropos) which we have made publicly available within ANTs.

**N4 bias correction.** Critical to quantitative processing of MRI is the minimization of field inhomogeneity effects which produce artificial low frequency intensity variation across the image. Large-scale studies, such as ADNI, employ perhaps the most widely used bias correction algorithm, N3 [36], as part of their standard protocol [37]. In [38] we introduced an improvement of N3, denoted as “N4”, which demonstrates a significant increase in performance and convergence behavior on a variety of data. This improvement is a result of an enhanced fitting routine (which includes multi-resolution capabilities) and a modified optimization formulation.

**Joint label fusion for prior-based segmentation.** Joint label fusion (JLF) is the current state-of-the-art for propagating expert labelings from a reference atlas library onto new instances of unlabeled data. Image registration is used to align the atlas library (images + segmentations) to a common space. A statistical model is then used to combine the “guesses” from all the normalized atlas labels to provide a “best guess” estimate of the target labeling. Several such algorithms have been developed and much effort has been devoted to determining relative performance levels. See, for example, the recent MICCAI 2012 Grand Challenge and Workshop on Multi-Atlas Labeling). The joint fusion (JLF) algorithm of [39, 40] is one of the top performing JLF algorithms. JLF is capable of predicting anatomical labels with accuracy that rivals expert anatomists [41]. It has proven its effectiveness in lung [42], cardiac data [43], the human brain [12], and in multiple modality canine MRI [43].

**Spatially adaptive denoising.** Patch-based denoising is critical for data “cleaning” prior to subsequent processing such as segmentation or spatial normalization. Recently, a spatially adaptive approach to denoising was proposed in [44] which we implemented in ANTs. This filter performs well and is also relatively fast.

The previously described core tools, as well as several others, have been part of ANTs and ITK development efforts for more than a decade. And it was precisely the deficiency of publicly available tools within the neuroscience community that motivated the inception and continued development of ANTs. As a result, our team is well-recognized for our many open-source contributions including seminal contributions to the field of image registration outlined earlier. Indeed, ANTs-based image registration serves as the basis for the registration component of the latest version of the National Library of Medicine Insight Toolkit (ITK) programming library (<http://www.itk.org>). The combination of state-of-the-art algorithms and feature-rich flexibility has translated to top-placed rankings in major independent evaluations for certain elements of the ANTs toolkit:

- SyN was a top performer in a fairly recent large-scale brain normalization evaluation [45].
- SyN also competed in the Evaluation of Methods for Pulmonary Image REGistration 2010 (EMPIRE10) challenge [46] where it was the top performer for the benchmarks used to assess lung registration accuracy and biological plausibility of the inferred transform (i.e., boundary alignment, fissure alignment, landmark correspondence, and displacement field topology).
- The joint label fusion algorithm of [39, 47] (coupled with SyN) performed well in the MICCAI 2012 challenge for labeled brain data [48] and in 2013 for labeled canine hind leg data [49].
- The multivariate template capabilities in ANTs were combined with random forests to win the Brain Tumor segmentation (BRATS) competition at MICCAI 2013 [18].
- A B-spline variant of the SyN algorithm [11] won the best paper award at the STACOM 2014 workshop for cardiac motion estimation [50].

### 3(c.1.2) ANTs and the neuroimaging community

ANTs takes advantage of the mature Insight ToolKit in providing an optimal software framework for building scripts and programs specifically for neuroimaging. For example, the following core neuroimage processing algorithms have been made available through our ANTs toolkit (complete with online self-contained examples with developer-tuned parameters) and have been used extensively by our group and others:

- brain normalization [51, 52] (<https://github.com/stnava/BasicBrainMapping>),
- brain template generation [17] (<https://github.com/ntustison/TemplateBuildingExample>),

- skull-stripping or brain extraction [12, 53] (<https://github.com/ntustison/antsBrainExtractionExample>),
- prior-based brain tissue segmentation [51] (<https://github.com/ntustison/antsAtroposN4Example>),
- cortical thickness estimation [12, 54] (<https://github.com/ntustison/antsCorticalThicknessExample>),
- brain tumor segmentation [18] (<https://github.com/ntustison/ANTsAndArboles>), and
- cortical labeling [39, 47] (<https://github.com/ntustison/MalfLabelingExample>).

All of these tools have been wrapped in easy-to-use, well-documented shell scripts. For example, the ANTs cortical thickness pipeline, as outlined in [12], comprises four major steps: (1) bias correction, (2) brain extraction, (3) *n*-tissue segmentation, and (4) cortical thickness estimation. Each step requires its own set of ANTs tools with appropriately tuned parameters. To maximize the utility of the pipeline for the interested user, in [12] we provide all the necessary programs (properly tuned) with a minimal set of input data required to obtain good results for common data. The result is an easy-to-use script that can be invoked by the programmer and non-programmer alike to obtain the desired processed data which outperforms the current state-of-the-art. This is an example command call for the ANTs cortical thickness pipeline:

```
# ANTs processing call for a single subject

$ sh antsCorticalThickness.sh -d 3 \
    -a IXI/T1/IXI002-Guys-0828-T1.nii.gz \
    -e IXI/template/T_Template0.nii.gz \
    -m IXI/template/T_template0ProbabilityMask.nii.gz \
    -f IXI/template/T_template0ExtractionMask.nii.gz \
    -p IXI/template/Priors/priors%d.nii.gz \
    -o IXI/ANTSResults/IXI002-Guys-02828-
```

This approach to reducing the steep learning curve associated with many processing pipelines has several benefits. Bash is an extremely common command language that permits large-scale processing. Thus, running several jobs on a cluster infrastructure is straightforward with this approach (as opposed to a GUI-driven processing paradigm). Such scripts are readable by the interested user who can glean parameters as well as manually make changes.

### **3(c.1.3) The significance of ANTs for the pulmonary imaging community**

Analogously, several algorithmic categories exist for lung image analysis which, as we have stated previously, do not exist in any comprehensive, publicly available package. This is in spite of the fact that new algorithms for lung image analysis are frequently reported in the literature. An extensive survey concentrating on the years 1999–2004 is given in [55] which covers computer-aided diagnosis of lung disease and lung cancer in CT (i.e., detection and tracking of pulmonary nodules) and provides an overview of the many relevant segmentation methods for pulmonary structures. Although many algorithms existed at the time, continued technical development has only increased the number of available algorithms. However, despite the continued reporting of pulmonary image analysis algorithms, there is no corresponding increase in algorithmic availability.

*A primary assumption for this proposal is that, through extension and continued development of ANTs and ITK functionality, we can make a significant impact for the pulmonary imaging research community in both basic science and clinical workflows by developing lung-specific algorithms which are easy to use as we have done for the neuroimaging community.* The following is a small sampling of more recently reported techniques for CT analysis that would be incorporated into ITK-Lung:

- whole lung differentiation from the chest wall (e.g., [56–59]),
- bronchial structure extraction (e.g., [60, 61] and the many submissions to the recent Extraction of Airways from CT (ExACT) challenge of the 2nd International Workshop on Pulmonary Image Analysis [62]),
- vasculature segmentation (e.g., [63, 64]),
- lobe and/or fissure detection (e.g., [65, 66]),
- feature extraction and classification (e.g., [67–69]), and
- nodule detection (e.g., [70] and the many submissions to the Automatic Nodule Detection (ANODE09) challenge of the 2009 CAD Conference of SPIE Medical Imaging [71]).

Although this list is restricted to CT image analysis, inclusion of additional techniques specific to other modalities has additional benefit and are included in this proposal. Using ANTs core tools, we have produced several lung-specific algorithms for core tasks:

**Atlas-based lung segmentation.** Identification of anatomical structure in MRI is often a crucial preprocessing step for quantification of morphological features or ventilation information from functional images. Quantitative regional analysis often requires the identification of lung and lobar anatomy. Although much algorithmic research for lung segmentation has been reported in the CT literature [72], co-opting such technologies is complicated by MRI-specific issues such as RF coil inhomogeneity, presence and resolution of structural detail, and the absence of a physically-based intensity scaling.

We recently proposed a multi-atlas approach for automatically segmenting the left and right lungs in proton MRI [42]. Multi-atlas approaches to segmentation have proven highly successful in neuroimaging [39, 47] and these methods translate readily to the pulmonary domain. Whereas many current strategies for lung image segmentation employ low-level processing techniques based on encodable heuristics, consensus-based strategies, in contrast, optimize the prior knowledge applied to a specific segmentation problem (cf Figure 3). The evaluation of our proposed method [42] demonstrated good performance with Jaccard overlap measures for the left and right lungs being  $0.966 \pm 0.018$  and  $0.970 \pm 0.016$ , respectively. One of the benefits of this approach is that it can also be applied effectively to pulmonary CT.

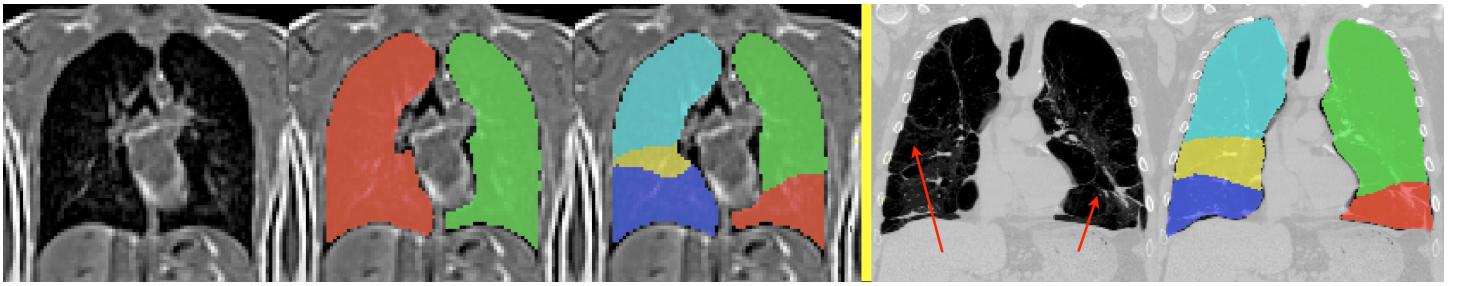


Figure 3: Sample lung and lobe estimation results in both proton MRI and CT using our atlas-based strategy. (Left) Lung segmentation and lobe estimation results for the given proton MRI. Although lobe estimation is dependent solely on the warped atlases, we are able to obtain accurate estimates of lobes which are useful for more regional analysis and provide a more intuitive and universal subdivision of the lungs than previous partitioning schemes. (Right) The utility of this method extends to CT where the integrity of lobar anatomical markers (such as the lack of fissures illustrated by the red arrows) have been compromised due to disease.

**Atlas-based lobe estimation.** For regional investigation of certain lung pathologies and conditions, it is often useful to quantify measurements of interest within more localized regions, such as the lobes. However there is little (if any) usable information in proton MRI for image-based lobar segmentation which has led to alternative geometric subdivisions which are ad hoc, non-anatomical, and do not adequately address intra- and inter-subject correspondences. However, we can take advantage of inter-subject similarities in lobar geometry to provide a prior-based estimation of lobar divisions using a consensus labeling approach (cf Figure 3).

To generate the lobe segmentation in a target proton or CT lung image, we first generate the binary whole lung mask using the whole lung atlas-based estimation. We then register the set of CT lung masks which have been expertly annotated to the target binary lung mask using the B-spline SyN registration approach described earlier [11]. Subsequently, we warp the set of CT lobe labels to the target image using the CT mask-to-target mask transformation. Since we have no intensity information inside the target lung mask and CT atlas lung masks, we use a simple majority voting strategy to generate the optimal labeling for the target image. Following the majority voting, we remove any labelings outside the lung mask and assign any unlabeled voxels with the label closest in distance to that voxel. This methodology is more thoroughly described in [42] where we showed that lobar overlap measures in proton MRI were on par with the state-of-the-art CT methods where fissure information is actually visible (left upper:  $0.882 \pm 0.059$ , left lower:  $0.868 \pm 0.06$ , right upper:  $0.852 \pm 0.067$ , right middle:  $0.657 \pm 0.130$ , right lower:  $0.873 \pm 0.063$ ).

**Ventilation quantification.** Automated or semiautomated approaches for classifying areas of varying degrees of ventilation are of potential benefit for pulmonary functional analysis. In [34], we presented an automated algorithmic pipeline for ventilation-based partitioning of the lungs in hyperpolarized  $^3\text{He}$  and  $^{129}\text{Xe}$  MRI. Without ground truth data for evaluation, we used a consensus labeling approach [73] to simultaneously estimate the true segmentation from given “raters” which included

the segmentation from our automated approach and the manual tracings of three trained individuals. In terms of combined specificity and sensitivity, our automated algorithm demonstrated superior performance with the added benefit of being reproducible and less time-consuming.

Since the initial development, we have continued to improve this segmentation pipeline by incorporating an iterative bias-correction/segmentation estimation scheme. An additional component that improves results is an ANTs-based implementation of the patch-based denoising protocol described in [44]. Example longitudinal segmentation results are provided in Figure 4.

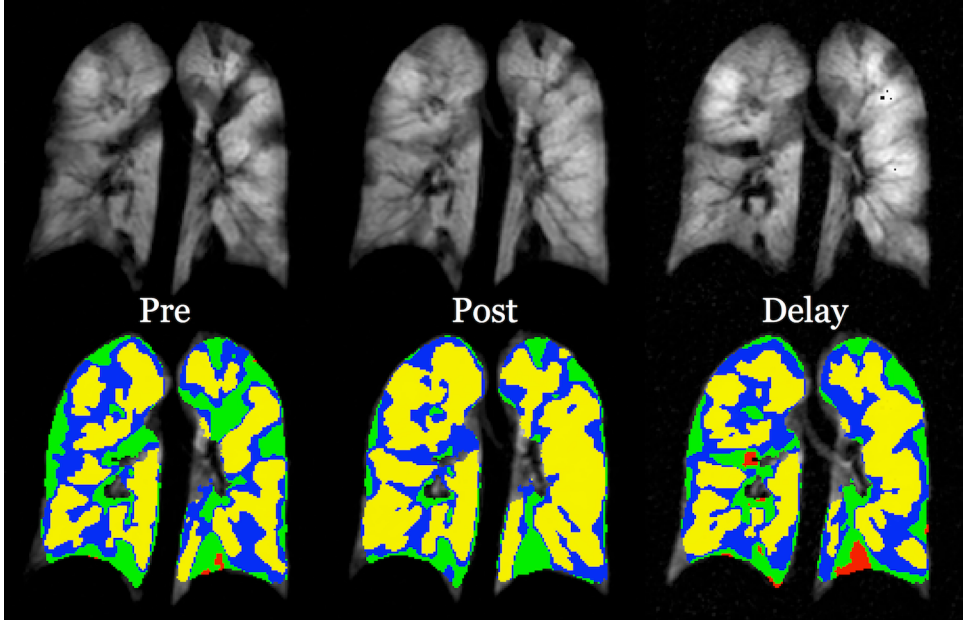


Figure 4: Pulmonary functional segmentation using the algorithmic framework first described in [34] for hyperpolarized  $^3\text{He}$  MRI. These data were taken from a current study looking at the implications in ventilation pre- and post-albuterol intake including an additional acquisition at some delay period following the post-albuterol imaging. The ventilation-based segmentation is as follows: red = no ventilation, green = poorly ventilated, blue = normally ventilated, and yellow = well-ventilated. Note the improvement in both the qualitative assessment of the ventilation map (top) and the corresponding segmentation time course (bottom) followed by an approximate return to pre-albuterol conditions following the delay period.

**Multi-modal lung template construction.** Additionally, although the template construction algorithm described in [17] is, as pointed out earlier, frequently applied to T1-weighted brain data, it is sufficiently generic such that it can also be applied to pulmonary data. Also, new innovations in diffeomorphic registration technology has led to a Symmetric Normalization B-spline variant which has demonstrated accurate normalizations [11] and transformations which are particularly well-suited for pulmonary data [74].

In Figure 4, we illustrate the major processing components of a recent study analyzing local changes based on a pulmonary treatment plan [75]. This study employed several of the tools we are proposing for inclusion in the specified aims. The first major component is the construction of a single-subject  $^3\text{He}/\text{proton}$  MRI template for all five imaging time points. This step generates the statistical coordinate system for the voxelwise regression analysis of the normalized intensities to determine correlation with expected treatment effects.

**Quantitative CT indices.** Imaging biomarkers for characterizing emphysema in CT have been well researched, although there are ample opportunities to refine these methods as well as to introduce more advanced approaches. Examples of the latter include texture analysis for identifying the centrilobular and groundglass opacities and fractal and connectivity approaches to differentiate centrilobular from panlobular emphysema. The indices for CT image analysis can roughly be divided into those that characterize the pulmonary parenchyma: volumetric tissue (e.g., [76, 77]), distribution of low attenuation areas (LAA) (e.g., [78, 79]), cooccurrence and run-length matrix features (e.g., [67, 80]), attenuation statistics (e.g., [81, 82]), deformation measures (e.g., [83, 84]), and stochastic fractal dimension features (e.g., [67, 82]) and those that characterize the airways (e.g., [85–87]).

The former are important for subjects with an emphysematous component of disease, whereas the latter are important for subjects with a bronchitic component of disease. An important premise of this proposal is that many of these measurements

## Longitudinal voxelwise analysis of ventilation data

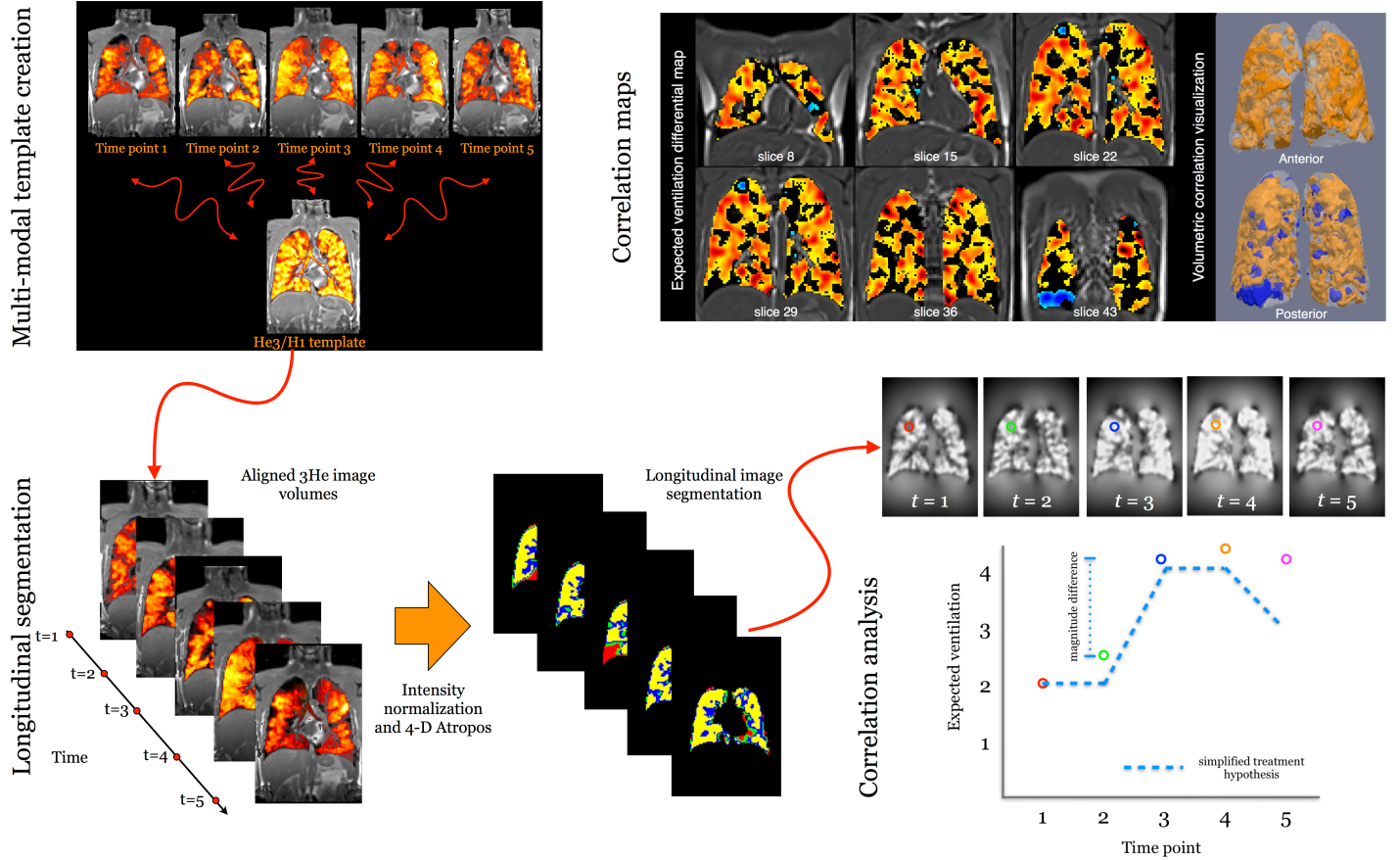


Figure 5: Voxelwise regression analysis to determine image-based response to treatment. First, a multi-modal, single-subject template is created to bring all time point images to the same coordinate system. 4-D segmentation is performed on the longitudinal time series of 3-D image volumes. Treatment effects are expected to follow the simplified treatment hypothesis illustrated with the dashed blue line in the plot on the right. To explore how the longitudinal change in expected ventilation follows this treatment hypothesis with image data, we smooth the aligned expected ventilation maps (to account for potential voxelwise misalignments) and then quantify how the voxelwise intensities regress with the simplified treatment hypothesis. This quantification is visualized using the correlation maps depicted in the template space (top right). Positive correlations with the expected treatment effect are rendered in orange whereas negative correlations are rendered in blue.

Volumetric Tissue Indices	Cooccurrence Matrix Texture Indices	Attenuation Histogram Statistics
lung volume lobar volume surface area surface area to volume ratio total lung weight tissue/airspace volumes of lung inspiration vs. expiration*	energy inertia contrast entropy correlation inverse difference moment cluster shade* cluster prominence* Haralick's correlation*	attenuation mean attenuation variance attenuation skewness attenuation kurtosis attenuation grey level entropy regional variants inspiration vs. expiration
Airway Indices		Deformation Indices
airway luminal diameter and area airway wall thickness percentage wall area thickness to diameter ratio airway branch angles airway segment length airway wall volumes (segmental and total)* inspiration vs. expiration		Jacobian of lung displacement lung deformation strain
Run-length Matrix Texture Indices		Stochastic Fractal Image Statistics
	short run emphasis long run emphasis grey level non-uniformity run-length non-uniformity run percentage low grey level run emphasis* high grey level run emphasis* short run low grey level emphasis* short high grey level run emphasis* long run low grey level emphasis* long high grey level run emphasis* inspiration vs. expiration*	mean variance skewness kurtosis grey level entropy inspiration vs. expiration*
Distribution of LAA Heterogeneity		Attenuation Mask Indices
10 partitions (std of 15 <sup>th</sup> %) slopes of density mask curves % size distribution of LAA areas volumetric cluster analysis inner core vs. outer rind inspiration vs. expiration*		HU density mask % HU density mask inspiration vs. expiration*

Table 1: Quantitative CT indices proposed for inclusion in the lung image analysis pipeline. Whole lung, regional, and voxelwise measurements are included, as well as population-based comparisons and longitudinal analysis of all indices. Indices marked with a '\*' denote novel measures which have not been previously utilized in chronic lung disease assessment but have shown classification capability in other application domains.

can also be directly applied to discriminative analysis using <sup>3</sup>He MRI for a variety of lung diseases. These indices can also be studied not only at any particular single time point, but also for changes with time. The addition of quantitative morphologic measurements of the airways provides an assessment of the contribution of airway changes to chronic lung disease.

Table 1 provides an overview of these types of discriminative measurements that can be used for CT and <sup>3</sup>He lung assessment. We have already implemented many of these image features and have contributed the result of our work to the Insight Toolkit (ITK) of the National Institutes of Health (e.g., [88, 89]). As an open-source repository for medical image analysis algorithms, contribution of our work to the ITK allows researchers full access to the latest image analysis algorithms in addition to avoiding research redundancy. It is also beneficial in that the entire ITK community participates in the vetting of the software library.

**3(c.2) Specific Aim 1:** To develop a set of open-source software tools for CT, proton, and  $^3\text{He}$  pulmonary computational analysis.

**3(c.3) Specific Aim 2.** To provide multiple sets of multi-modal annotated lung data (CT, proton, and  $^3\text{He}$ ) for public use.

**3(c.4) Specific Aim 3.** Evaluate and disseminate multiple complete studies with input data from multiple investigators to showcase the utility of the tools and data provided with this proposal.

#### **Anticipated difficulties**

Signal intensity in the lungs is poor in areas of low ventilation. COPD and asthma are obstructive lung diseases which exhibit focal areas of decreased signal intensity on  $^3\text{He}$  MRI which are thought to correspond to areas of reduced ventilation. These ventilation defects severely inhibit our ability to detect the lung boundaries for proper segmentation. Also, most of the COPD and asthmatic patients will have ventilation defects with the moderate asthmatics having greater than 1 defect per slice also negatively affecting boundary delineation. Note that there are similar issues for CT images of severe pathologies. However, given the shape and intensity prior statistics contained by our  $^3\text{He}$  MRI and CT lung templates, it is expected that the templates, in combination with our proposed segmentation algorithms, will be sufficient to provide a good initialization for subsequent manual segmentation if they do not yield an adequate segmentation result. The CT data, which provides excellent contrast between the lung and chest wall, can also be used to inform the  $^3\text{He}$  MRI segmentation.

## References

1. Wang, Y.-X. and Deng, M. “**Medical Imaging in New Drug Clinical Development**” *J Thorac Dis* 2, no. 4 (2010): 245–52. doi:[10.3978/j.issn.2072-1439.2010.11.10](https://doi.org/10.3978/j.issn.2072-1439.2010.11.10)
2. Zhao, B., Tan, Y., Bell, D. J., Marley, S. E., Guo, P., Mann, H., Scott, M. L. J., Schwartz, L. H., and Ghiorghiu, D. C. “**Exploring Intra- and Inter-Reader Variability in Uni-Dimensional, Bi-Dimensional, and Volumetric Measurements of Solid Tumors on CT Scans Reconstructed at Different Slice Intervals**” *Eur J Radiol* 82, no. 6 (2013): 959–68. doi:[10.1016/j.ejrad.2013.02.018](https://doi.org/10.1016/j.ejrad.2013.02.018)
3. McErlean, A., Panicek, D. M., Zabor, E. C., Moskowitz, C. S., Bitar, R., Motzer, R. J., Hricak, H., and Ginsberg, M. S. “**Intra- and Interobserver Variability in CT Measurements in Oncology**” *Radiology* 269, no. 2 (2013): 451–9. doi:[10.1148/radiol.13122665](https://doi.org/10.1148/radiol.13122665)
4. Fischl, B. “**FreeSurfer**” *Neuroimage* 62, no. 2 (2012): 774–81. doi:[10.1016/j.neuroimage.2012.01.021](https://doi.org/10.1016/j.neuroimage.2012.01.021)
5. Jenkinson, M., Beckmann, C. F., Behrens, T. E. J., Woolrich, M. W., and Smith, S. M. “**FSL**” *Neuroimage* 62, no. 2 (2012): 782–90. doi:[10.1016/j.neuroimage.2011.09.015](https://doi.org/10.1016/j.neuroimage.2011.09.015)
6. Cox, R. W. “**AFNI: what a Long Strange Trip It’s Been**” *Neuroimage* 62, no. 2 (2012): 743–7. doi:[10.1016/j.neuroimage.2011.08.025](https://doi.org/10.1016/j.neuroimage.2011.08.025)
7. Ashburner, J. “**SPM: a History**” *Neuroimage* 62, no. 2 (2012): 791–800. doi:[10.1016/j.neuroimage.2011.10.025](https://doi.org/10.1016/j.neuroimage.2011.10.025)
8. Hoffman, E. A., Lynch, D. A., Barr, R. G., Beek, E. J. R. van, Parraga, G., and IWPFI Investigators. “**Pulmonary CT and MRI Phenotypes That Help Explain Chronic Pulmonary Obstruction Disease Pathophysiology and Outcomes**” *J Magn Reson Imaging* (2015): doi:[10.1002/jmri.25010](https://doi.org/10.1002/jmri.25010)
9. Yunwen, Y. and Kishida, K. “**Toward an Understanding of the Motivation of Open Source Software Developers**” *Software engineering, 2003. proceedings. 25th international conference on* (2003): 419–429. doi:[10.1109/ICSE.2003.1201220](https://doi.org/10.1109/ICSE.2003.1201220)
10. (2008): Available at <http://fsmsh.com/2845>
11. Tustison, N. J. and Avants, B. B. “**Explicit B-Spline Regularization in Diffeomorphic Image Registration**” *Front Neuroinform* 7, (2013): 39. doi:[10.3389/fninf.2013.00039](https://doi.org/10.3389/fninf.2013.00039)
12. Tustison, N. J., Cook, P. A., Klein, A., Song, G., Das, S. R., Duda, J. T., Kandel, B. M., Strien, N. van, Stone, J. R., Gee, J. C., and Avants, B. B. “**Large-Scale Evaluation of ANTs and FreeSurfer Cortical Thickness Measurements**” *Neuroimage* 99, (2014): 166–79. doi:[10.1016/j.neuroimage.2014.05.044](https://doi.org/10.1016/j.neuroimage.2014.05.044)
13. Bajcsy, R. and Broit, C. “**Matching of Deformed Images**” *Sixth international conference on pattern recognition (iCPR’82)* (1982): 351–353.
14. Bajcsy, R. and Kovacic, S. “**Multiresolution Elastic Matching**” *Computer Vision, Graphics, and Image Processing* 46, no. 1 (1989): 1–21. doi:[10.1016/S0734-189X\(89\)80014-3](https://doi.org/10.1016/S0734-189X(89)80014-3), Available at [http://dx.doi.org/10.1016/S0734-189X\(89\)80014-3](http://dx.doi.org/10.1016/S0734-189X(89)80014-3)
15. Gee, J. C., Reivich, M., and Bajcsy, R. “**Elastically Deforming 3D Atlas to Match Anatomical Brain Images**” *J Comput Assist Tomogr* 17, no. 2 () 225–36.
16. Avants, B. B., Epstein, C. L., Grossman, M., and Gee, J. C. “**Symmetric Diffeomorphic Image Registration with Cross-Correlation: evaluating Automated Labeling of Elderly and Neurodegenerative Brain**” *Med Image Anal* 12, no. 1 (2008): 26–41. doi:[10.1016/j.media.2007.06.004](https://doi.org/10.1016/j.media.2007.06.004)
17. Avants, B. B., Yushkevich, P., Pluta, J., Minkoff, D., Koreckowski, M., Detre, J., and Gee, J. C. “**The Optimal Template Effect in Hippocampus Studies of Diseased Populations**” *Neuroimage* 49, no. 3 (2010): 2457–66. doi:[10.1016/j.neuroimage.2009.09.062](https://doi.org/10.1016/j.neuroimage.2009.09.062)
18. Tustison, N. J., Shrinidhi, K. L., Wintermark, M., Durst, C. R., Kandel, B. M., Gee, J. C., Grossman, M. C., and Avants, B. B. “**Optimal Symmetric Multimodal Templates and Concatenated Random Forests for Supervised Brain Tumor Segmentation (Simplified) with ANTsR**” *Neuroinformatics* (2014): doi:[10.1007/s12021-014-9245-2](https://doi.org/10.1007/s12021-014-9245-2)
19. Avants, B. B., Duda, J. T., Kilroy, E., Krasileva, K., Jann, K., Kandel, B. T., Tustison, N. J., Yan, L., Jog, M., Smith, R., Wang, Y., Dapretto, M., and Wang, D. J. J. “**The Pediatric Template of Brain Perfusion**” *Sci Data* 2, (2015): 150003. doi:[10.1038/sdata.2015.3](https://doi.org/10.1038/sdata.2015.3)

20. Datta, R., Lee, J., Duda, J., Avants, B. B., Vite, C. H., Tseng, B., Gee, J. C., Aguirre, G. D., and Aguirre, G. K. “**A Digital Atlas of the Dog Brain**” *PLoS One* 7, no. 12 (2012): e52140. doi:[10.1371/journal.pone.0052140](https://doi.org/10.1371/journal.pone.0052140)
21. McMillan, C. T., Avants, B. B., Cook, P., Ungar, L., Trojanowski, J. Q., and Grossman, M. “**The Power of Neuroimaging Biomarkers for Screening Frontotemporal Dementia**” *Hum Brain Mapp* 35, no. 9 (2014): 4827–40. doi:[10.1002/hbm.22515](https://doi.org/10.1002/hbm.22515)
22. Cook, P. A., McMillan, C. T., Avants, B. B., Peelle, J. E., Gee, J. C., and Grossman, M. “**Relating Brain Anatomy and Cognitive Ability Using a Multivariate Multimodal Framework**” *Neuroimage* 99, (2014): 477–86. doi:[10.1016/j.neuroimage.2014.09.030](https://doi.org/10.1016/j.neuroimage.2014.09.030)
23. Vannier, M. W., Butterfield, R. L., Jordan, D., Murphy, W. A., Levitt, R. G., and Gado, M. “**Multispectral Analysis of Magnetic Resonance Images**” *Radiology* 154, no. 1 (1985): 221–4. doi:[10.1148/radiology.154.1.3964938](https://doi.org/10.1148/radiology.154.1.3964938)
24. Dempster, A., Laird, N., and Rubin, D. “**Maximum Likelihood Estimation from Incomplete Data Using the EM Algorithms**” *Journal of the Royal Statistical Society* 39, (1977): 1–38.
25. Wells, W. M., Grimson, W. L., Kikinis, R., and Jolesz, F. A. “**Adaptive Segmentation of MRI Data**” *IEEE Trans Med Imaging* 15, no. 4 (1996): 429–42. doi:[10.1109/42.511747](https://doi.org/10.1109/42.511747)
26. Cline, H. E., Lorensen, W. E., Kikinis, R., and Jolesz, F. “**Three-Dimensional Segmentation of MR Images of the Head Using Probability and Connectivity**” *J Comput Assist Tomogr* 14, no. 6 (): 1037–45.
27. Kikinis, R., Shenton, M. E., Gerig, G., Martin, J., Anderson, M., Metcalf, D., Guttmann, C. R., McCarley, R. W., Lorensen, W., and Cline, H. “**Routine Quantitative Analysis of Brain and Cerebrospinal Fluid Spaces with MR Imaging**” *J Magn Reson Imaging* 2, no. 6 (): 619–29.
28. Geman, S. and Geman, D. “**Stochastic Relaxation, Gibbs Distributions, and the Bayesian Restoration of Images**” *IEEE Trans Pattern Anal Mach Intell* 6, no. 6 (1984): 721–41.
29. Held, K., Rota Kops, E., Krause, B. J., Wells, W. M., 3rd, Kikinis, R., and Müller-Gärtner, H. W. “**Markov Random Field Segmentation of Brain MR Images**” *IEEE Trans Med Imaging* 16, no. 6 (1997): 878–86. doi:[10.1109/42.650883](https://doi.org/10.1109/42.650883)
30. Van Leemput, K., Maes, F., Vandermeulen, D., and Suetens, P. “**Automated Model-Based Tissue Classification of MR Images of the Brain**” *IEEE Trans Med Imaging* 18, no. 10 (1999): 897–908. doi:[10.1109/42.811270](https://doi.org/10.1109/42.811270)
31. Ashburner, J. and Friston, K. J. “**Unified Segmentation**” *Neuroimage* 26, no. 3 (2005): 839–51. doi:[10.1016/j.neuroimage.2005.02.031](https://doi.org/10.1016/j.neuroimage.2005.02.031)
32. Gubern-Mérida, A., Kallenberg, M., Mann, R. M., Martí, R., and Karssemeijer, N. “**Breast Segmentation and Density Estimation in Breast MRI: a Fully Automatic Framework**” *IEEE J Biomed Health Inform* 19, no. 1 (2015): 349–57. doi:[10.1109/JBHI.2014.2311163](https://doi.org/10.1109/JBHI.2014.2311163)
33. Ribes, S., Didierlaurent, D., Decoster, N., Gonneau, E., Risser, L., Feillel, V., and Caselles, O. “**Automatic Segmentation of Breast MR Images Through a Markov Random Field Statistical Model**” *IEEE Trans Med Imaging* 33, no. 10 (2014): 1986–96. doi:[10.1109/TMI.2014.2329019](https://doi.org/10.1109/TMI.2014.2329019)
34. Tustison, N. J., Avants, B. B., Flors, L., Altes, T. A., Lange, E. E. de, Mugler, J. P., 3rd, and Gee, J. C. “**Ventilation-Based Segmentation of the Lungs Using Hyperpolarized (3)He MRI**” *J Magn Reson Imaging* 34, no. 4 (2011): 831–41. doi:[10.1002/jmri.22738](https://doi.org/10.1002/jmri.22738)
35. Avants, B. B., Tustison, N. J., Wu, J., Cook, P. A., and Gee, J. C. “**An Open Source Multivariate Framework for n-Tissue Segmentation with Evaluation on Public Data**” *Neuroinformatics* 9, no. 4 (2011): 381–400. doi:[10.1007/s12021-011-9109-y](https://doi.org/10.1007/s12021-011-9109-y)
36. Sled, J. G., Zijdenbos, A. P., and Evans, A. C. “**A Nonparametric Method for Automatic Correction of Intensity Nonuniformity in MRI Data**” *IEEE Trans Med Imaging* 17, no. 1 (1998): 87–97. doi:[10.1109/42.668698](https://doi.org/10.1109/42.668698)
37. Boyes, R. G., Gunter, J. L., Frost, C., Janke, A. L., Yeatman, T., Hill, D. L. G., Bernstein, M. A., Thompson, P. M., Weiner, M. W., Schuff, N., Alexander, G. E., Killiany, R. J., DeCarli, C., Jack, C. R., Fox, N. C., and ADNI Study. “**Intensity Non-Uniformity Correction Using N3 on 3-T Scanners with Multichannel Phased Array Coils**” *Neuroimage* 39, no. 4 (2008): 1752–62. doi:[10.1016/j.neuroimage.2007.10.026](https://doi.org/10.1016/j.neuroimage.2007.10.026)
38. Tustison, N. J., Awate, S. P., Cai, J., Altes, T. A., Miller, G. W., Lange, E. E. de, Mugler, J. P., 3rd, and Gee, J. C. “**Pulmonary Kinematics from Tagged Hyperpolarized Helium-3 MRI**” *J Magn Reson Imaging* 31, no. 5 (2010): 1236–41. doi:[10.1002/jmri.22137](https://doi.org/10.1002/jmri.22137)

39. Wang, H. and Yushkevich, P. A. “**Multi-Atlas Segmentation with Joint Label Fusion and Corrective Learning-an Open Source Implementation**” *Front Neuroinform* 7, (2013): 27. doi:[10.3389/fninf.2013.00027](https://doi.org/10.3389/fninf.2013.00027)
40. Wang, H., Suh, J. W., Das, S. R., Pluta, J. B., Craige, C., and Yushkevich, P. A. “**Multi-Atlas Segmentation with Joint Label Fusion**” *IEEE Trans Pattern Anal Mach Intell* 35, no. 3 (2013): 611–23. doi:[10.1109/TPAMI.2012.143](https://doi.org/10.1109/TPAMI.2012.143)
41. Yushkevich, P. A., Wang, H., Pluta, J., Das, S. R., Craige, C., Avants, B. B., Weiner, M. W., and Mueller, S. “**Nearly Automatic Segmentation of Hippocampal Subfields in in Vivo Focal T2-Weighted MRI**” *Neuroimage* 53, no. 4 (2010): 1208–24. doi:[10.1016/j.neuroimage.2010.06.040](https://doi.org/10.1016/j.neuroimage.2010.06.040)
42. Tustison, N. J., Qing, K., Wang, C., Altes, T. A., and Mugler, J. P., 3rd. “**Atlas-Based Estimation of Lung and Lobar Anatomy in Proton MRI**” *Magn Reson Med* (Accepted):
43. Available at [https://masi.vuse.vanderbilt.edu/workshop2013/index.php/Main\\_Page](https://masi.vuse.vanderbilt.edu/workshop2013/index.php/Main_Page)
44. Manjón, J. V., Coupé, P., Martí-Bonmatí, L., Collins, D. L., and Robles, M. “**Adaptive Non-Local Means Denoising of MR Images with Spatially Varying Noise Levels**” *J Magn Reson Imaging* 31, no. 1 (2010): 192–203. doi:[10.1002/jmri.22003](https://doi.org/10.1002/jmri.22003)
45. Klein, A., Andersson, J., Ardekani, B. A., Ashburner, J., Avants, B., Chiang, M.-C., Christensen, G. E., Collins, D. L., Gee, J., Hellier, P., Song, J. H., Jenkinson, M., Lepage, C., Rueckert, D., Thompson, P., Vercauteren, T., Woods, R. P., Mann, J. J., and Parsey, R. V. “**Evaluation of 14 Nonlinear Deformation Algorithms Applied to Human Brain MRI Registration**” *Neuroimage* 46, no. 3 (2009): 786–802. doi:[10.1016/j.neuroimage.2008.12.037](https://doi.org/10.1016/j.neuroimage.2008.12.037)
46. Murphy, K., Ginneken, B. van, Reinhardt, J. M., Kabus, S., Ding, K., Deng, X., Cao, K., Du, K., Christensen, G. E., Garcia, V., Vercauteren, T., Ayache, N., Commowick, O., Malandain, G., Glocker, B., Paragios, N., Navab, N., Gorbunova, V., Sporrung, J., Bruijne, M. de, Han, X., Heinrich, M. P., Schnabel, J. A., Jenkinson, M., Lorenz, C., Modat, M., McClelland, J. R., Ourselin, S., Muenzing, S. E. A., Viergever, M. A., De Nigris, D., Collins, D. L., Arbel, T., Peroni, M., Li, R., Sharp, G. C., Schmidt-Richberg, A., Ehrhardt, J., Werner, R., Smeets, D., Loeckx, D., Song, G., Tustison, N., Avants, B., Gee, J. C., Staring, M., Klein, S., Stoel, B. C., Urschler, M., Werlberger, M., Vandemeulebroucke, J., Rit, S., Sarrut, D., and Pluim, J. P. W. “**Evaluation of Registration Methods on Thoracic CT: the EMPIRE10 Challenge**” *IEEE Trans Med Imaging* 30, no. 11 (2011): 1901–20. doi:[10.1109/TMI.2011.2158349](https://doi.org/10.1109/TMI.2011.2158349)
47. Wang, H., Suh, J. W., Das, S. R., Pluta, J., Craige, C., and Yushkevich, P. A. “**Multi-Atlas Segmentation with Joint Label Fusion**” *IEEE Trans Pattern Anal Mach Intell* (2012): doi:[10.1109/TPAMI.2012.143](https://doi.org/10.1109/TPAMI.2012.143)
48. “**MICCAI 2012 Workshop on Multi-Atlas Labeling**” (2012):
49. Asman, A., Akhondi-Asl, A., Wang, H., Tustison, N., Avants, B., Warfield, S. K., and Landman, B. “**MICCAI 2013 Segmentation Algorithms, Theory and Applications (SATA) Challenge Results Summary**,” *MICCAI 2013 challenge workshop on segmentation: Algorithms, theory and applications*. (2013):
50. Tustison, N. J., Yang, Y., and Salerno, M. “**Advanced Normalization Tools for Cardiac Motion Correction**” *Statistical atlases and computational models of the heart - imaging and modelling challenges* 8896, (2015): 3–12. doi:[10.1007/978-3-319-14678-2\\_1](https://doi.org/10.1007/978-3-319-14678-2_1), Available at [http://dx.doi.org/10.1007/978-3-319-14678-2\\_1](http://dx.doi.org/10.1007/978-3-319-14678-2_1)
51. Avants, B. B., Tustison, N. J., Song, G., Cook, P. A., Klein, A., and Gee, J. C. “**A Reproducible Evaluation of ANTs Similarity Metric Performance in Brain Image Registration**” *Neuroimage* 54, no. 3 (2011): 2033–44. doi:[10.1016/j.neuroimage.2010.09.025](https://doi.org/10.1016/j.neuroimage.2010.09.025)
52. Avants, B. B., Tustison, N. J., Stauffer, M., Song, G., Wu, B., and Gee, J. C. “**The Insight ToolKit Image Registration Framework**” *Front Neuroinform* 8, (2014): 44. doi:[10.3389/fninf.2014.00044](https://doi.org/10.3389/fninf.2014.00044)
53. Avants, B. B., Klein, A., Tustison, N. J., Woo, J., and Gee, J. C. “**Evaluation of Open-Access, Automated Brain Extraction Methods on Multi-Site Multi-Disorder Data**” *16th annual meeting for the organization of human brain mapping* (2010):
54. Das, S. R., Avants, B. B., Grossman, M., and Gee, J. C. “**Registration Based Cortical Thickness Measurement**” *Neuroimage* 45, no. 3 (2009): 867–79. doi:[10.1016/j.neuroimage.2008.12.016](https://doi.org/10.1016/j.neuroimage.2008.12.016)
55. Sluimer, I., Schilham, A., Prokop, M., and Ginneken, B. van. “**Computer Analysis of Computed Tomography Scans of the Lung: a Survey**” *IEEE Trans Med Imaging* 25, no. 4 (2006): 385–405. doi:[10.1109/TMI.2005.862753](https://doi.org/10.1109/TMI.2005.862753)

56. De Nunzio, G., Tommasi, E., Agrusti, A., Cataldo, R., De Mitri, I., Favetta, M., Maglio, S., Massafra, A., Quarta, M., Torsello, M., Zecca, I., Bellotti, R., Tangaro, S., Calvini, P., Camarlinghi, N., Falaschi, F., Cerello, P., and Oliva, P. “**Automatic Lung Segmentation in CT Images with Accurate Handling of the Hilar Region**” *J Digit Imaging* 24, no. 1 (2011): 11–27. doi:[10.1007/s10278-009-9229-1](https://doi.org/10.1007/s10278-009-9229-1)
57. Prasad, M. N., Brown, M. S., Ahmad, S., Abtin, F., Allen, J., Costa, I. da, Kim, H. J., McNitt-Gray, M. F., and Goldin, J. G. “**Automatic Segmentation of Lung Parenchyma in the Presence of Diseases Based on Curvature of Ribs**” *Acad Radiol* 15, no. 9 (2008): 1173–80. doi:[10.1016/j.acra.2008.02.004](https://doi.org/10.1016/j.acra.2008.02.004)
58. Wang, J., Li, F., and Li, Q. “**Automated Segmentation of Lungs with Severe Interstitial Lung Disease in CT**” *Med Phys* 36, no. 10 (2009): 4592–9.
59. Rikxoort, E. M. van, Hoop, B. de, Viergever, M. A., Prokop, M., and Ginneken, B. van. “**Automatic Lung Segmentation from Thoracic Computed Tomography Scans Using a Hybrid Approach with Error Detection**” *Med Phys* 36, no. 7 (2009): 2934–47.
60. Zheng, B., Leader, J. K., McMurray, J. M., Park, S. C., Fuhrman, C. R., Gur, D., and Sciurba, F. C. “**Automated Detection and Quantitative Assessment of Pulmonary Airways Depicted on CT Images**” *Med Phys* 34, no. 7 (2007): 2844–52.
61. Nakamura, M., Wada, S., Miki, T., Shimada, Y., Suda, Y., and Tamura, G. “**Automated Segmentation and Morphometric Analysis of the Human Airway Tree from Multidetector CT Images**” *J Physiol Sci* 58, no. 7 (2008): 493–8. doi:[10.2170/physiolsci.RP007408](https://doi.org/10.2170/physiolsci.RP007408)
62. Lo, P., Ginneken, B. van, Reinhardt, J. M., and Bruijne, M. de. “**Extraction of Airways from CT (EXACT '09)**” *The second international workshop on pulmonary image analysis* (2009):
63. Agam, G., Armato, S. G., 3rd, and Wu, C. “**Vessel Tree Reconstruction in Thoracic CT Scans with Application to Nodule Detection**” *IEEE Trans Med Imaging* 24, no. 4 (2005): 486–99.
64. Korfiatis, P. D., Kalogeropoulou, C., Karahaliou, A. N., Kazantzi, A. D., and Costaridou, L. I. “**Vessel Tree Segmentation in Presence of Interstitial Lung Disease in MDCT**” *IEEE Trans Inf Technol Biomed* 15, no. 2 (2011): 214–20. doi:[10.1109/TITB.2011.2112668](https://doi.org/10.1109/TITB.2011.2112668)
65. Qi, S., Triest, H. J. W. van, Yue, Y., Xu, M., and Kang, Y. “**Automatic Pulmonary Fissure Detection and Lobe Segmentation in CT Chest Images**” *Biomed Eng Online* 13, (2014): 59. doi:[10.1186/1475-925X-13-59](https://doi.org/10.1186/1475-925X-13-59)
66. Doel, T., Gavaghan, D. J., and Grau, V. “**Review of Automatic Pulmonary Lobe Segmentation Methods from CT**” *Comput Med Imaging Graph* 40, (2015): 13–29. doi:[10.1016/j.compmedimag.2014.10.008](https://doi.org/10.1016/j.compmedimag.2014.10.008)
67. Uppaluri, R., Hoffman, E. A., Sonka, M., Hartley, P. G., Hunninghake, G. W., and McLennan, G. “**Computer Recognition of Regional Lung Disease Patterns**” *Am J Respir Crit Care Med* 160, no. 2 (1999): 648–54. doi:[10.1164/ajrccm.160.2.9804094](https://doi.org/10.1164/ajrccm.160.2.9804094)
68. Rosas, I. O., Yao, J., Avila, N. A., Chow, C. K., Gahl, W. A., and Gochuico, B. R. “**Automated Quantification of High-Resolution CT Scan Findings in Individuals at Risk for Pulmonary Fibrosis**” *Chest* 140, no. 6 (2011): 1590–7. doi:[10.1378/chest.10-2545](https://doi.org/10.1378/chest.10-2545)
69. DeBoer, E. M., Swiercz, W., Heltshe, S. L., Anthony, M. M., Szeffler, P., Klein, R., Strain, J., Brody, A. S., and Sagel, S. D. “**Automated CT Scan Scores of Bronchiectasis and Air Trapping in Cystic Fibrosis**” *Chest* 145, no. 3 (2014): 593–603. doi:[10.1378/chest.13-0588](https://doi.org/10.1378/chest.13-0588)
70. Messay, T., Hardie, R. C., and Rogers, S. K. “**A New Computationally Efficient CAD System for Pulmonary Nodule Detection in CT Imagery**” *Med Image Anal* 14, no. 3 (2010): 390–406. doi:[10.1016/j.media.2010.02.004](https://doi.org/10.1016/j.media.2010.02.004)
71. Ginneken, B. van, Armato, S. G., 3rd, Hoop, B. de, Vorst, S. van Amelsvoort-van de, Duindam, T., Niemeijer, M., Murphy, K., Schilham, A., Retico, A., Fantacci, M. E., Camarlinghi, N., Bagagli, F., Gori, I., Hara, T., Fujita, H., Gargano, G., Bellotti, R., Tangaro, S., Bolaños, L., De Carlo, F., Cerello, P., Cristian Cheran, S., Lopez Torres, E., and Prokop, M. “**Comparing and Combining Algorithms for Computer-Aided Detection of Pulmonary Nodules in Computed Tomography Scans: The ANODE09 Study**” *Med Image Anal* 14, no. 6 (2010): 707–22. doi:[10.1016/j.media.2010.05.005](https://doi.org/10.1016/j.media.2010.05.005)
72. Rikxoort, E. M. van and Ginneken, B. van. “**Automated Segmentation of Pulmonary Structures in Thoracic Computed Tomography Scans: a Review**” *Phys Med Biol* 58, no. 17 (2013): R187–220. doi:[10.1088/0031-9155/58/17/R187](https://doi.org/10.1088/0031-9155/58/17/R187)

73. Warfield, S. K., Zou, K. H., and Wells, W. M. “**Simultaneous Truth and Performance Level Estimation (STAPLE): an Algorithm for the Validation of Image Segmentation**” *IEEE Trans Med Imaging* 23, no. 7 (2004): 903–21. doi:[10.1109/TMI.2004.828354](https://doi.org/10.1109/TMI.2004.828354)
74. Tustison, N. J., Song, G., Gee, James C, and Avants, B. B. “**Two Greedy SyN Variants for Pulmonary Image Registration**” *Evaluation of methods for pulmonary image registration (EMPIRE10)* (2012):
75. Tustison, N. J., Contrella, B., Altes, T. A., Avants, B. B., Lange, E. E. de, and Mugler, J. P. “**Longitudinal Assessment of Treatment Effects on Pulmonary Ventilation Using  $^{1}\text{H}/^{3}\text{He}$  MRI Multivariate Templates**” *Proc. SPIE 8672, medical imaging 2013: Biomedical applications in molecular, structural, and functional imaging* (2013):
76. Coxson, H. O., Rogers, R. M., Whittall, K. P., D'yachkova, Y., Paré, P. D., Sciurba, F. C., and Hogg, J. C. “**A Quantification of the Lung Surface Area in Emphysema Using Computed Tomography**” *Am J Respir Crit Care Med* 159, no. 3 (1999): 851–6. doi:[10.1164/ajrccm.159.3.9805067](https://doi.org/10.1164/ajrccm.159.3.9805067)
77. Perez, A., 4th, Coxson, H. O., Hogg, J. C., Gibson, K., Thompson, P. F., and Rogers, R. M. “**Use of CT Morphometry to Detect Changes in Lung Weight and Gas Volume**” *Chest* 128, no. 4 (2005): 2471–7. doi:[10.1378/chest.128.4.2471](https://doi.org/10.1378/chest.128.4.2471)
78. Coxson, H. O. and Rogers, R. M. “**New Concepts in the Radiological Assessment of COPD**” *Semin Respir Crit Care Med* 26, no. 2 (2005): 211–20. doi:[10.1055/s-2005-869540](https://doi.org/10.1055/s-2005-869540)
79. Stolk, J., Putter, H., Bakker, E. M., Shaker, S. B., Parr, D. G., Piitulainen, E., Russi, E. W., Grebski, E., Dirksen, A., Stockley, R. A., Reiber, J. H. C., and Stoel, B. C. “**Progression Parameters for Emphysema: a Clinical Investigation**” *Respir Med* 101, no. 9 (2007): 1924–30. doi:[10.1016/j.rmed.2007.04.016](https://doi.org/10.1016/j.rmed.2007.04.016)
80. Xu, Y., Sonka, M., McLennan, G., Guo, J., and Hoffman, E. A. “**MDCT-Based 3-D Texture Classification of Emphysema and Early Smoking Related Lung Pathologies**” *IEEE Trans Med Imaging* 25, no. 4 (2006): 464–75. doi:[10.1109/TMI.2006.870889](https://doi.org/10.1109/TMI.2006.870889)
81. Gevenois, P. A., De Vuyst, P., Sy, M., Scillia, P., Chaminade, L., Maertelaer, V. de, Zanen, J., and Yernault, J. C. “**Pulmonary Emphysema: quantitative CT During Expiration**” *Radiology* 199, no. 3 (1996): 825–9. doi:[10.1148/radiology.199.3.8638012](https://doi.org/10.1148/radiology.199.3.8638012)
82. Hoffman, E. A., Simon, B. A., and McLennan, G. “**State of the Art. a Structural and Functional Assessment of the Lung via Multidetector-Row Computed Tomography: phenotyping Chronic Obstructive Pulmonary Disease**” *Proc Am Thorac Soc* 3, no. 6 (2006): 519–32. doi:[10.1513/pats.200603-o86MS](https://doi.org/10.1513/pats.200603-o86MS)
83. Gee, J., Sundaram, T., Hasegawa, I., Uematsu, H., and Hatabu, H. “**Characterization of Regional Pulmonary Mechanics from Serial Magnetic Resonance Imaging Data**” *Acad Radiol* 10, no. 10 (2003): 1147–52.
84. Sundaram, T. A. and Gee, J. C. “**Towards a Model of Lung Biomechanics: pulmonary Kinematics via Registration of Serial Lung Images**” *Med Image Anal* 9, no. 6 (2005): 524–37. doi:[10.1016/j.media.2005.04.002](https://doi.org/10.1016/j.media.2005.04.002)
85. Aykac, D., Hoffman, E. A., McLennan, G., and Reinhardt, J. M. “**Segmentation and Analysis of the Human Airway Tree from Three-Dimensional X-Ray CT Images**” *IEEE Trans Med Imaging* 22, no. 8 (2003): 940–50. doi:[10.1109/TMI.2003.815905](https://doi.org/10.1109/TMI.2003.815905)
86. Park, W., Hoffman, E. A., and Sonka, M. “**Segmentation of Intrathoracic Airway Trees: a Fuzzy Logic Approach**” *IEEE Trans Med Imaging* 17, no. 4 (1998): 489–97. doi:[10.1109/42.730394](https://doi.org/10.1109/42.730394)
87. Ederle, J. R., Heussel, C. P., Hast, J., Fischer, B., Van Beek, E. J. R., Ley, S., Thelen, M., and Kauczor, H. U. “**Evaluation of Changes in Central Airway Dimensions, Lung Area and Mean Lung Density at Paired Inspiratory/Expiratory High-Resolution Computed Tomography**” *Eur Radiol* 13, no. 11 (2003): 2454–61. doi:[10.1007/s00330-003-1909-5](https://doi.org/10.1007/s00330-003-1909-5)
88. Tustison, N. J. and Gee, J. C. “**Run-Length Matrices for Texture Analysis**” *Insight Journal* (2008):
89. Tustison, N. J. and Gee, J. C. “**Stochastic Fractal Dimension Image**” *Insight Journal* (2009):